JOC The Journal of Organic Chemistry

Article

pubs.acs.org/joc

Internally versus Externally Solvated Derivatives of Doubly Bridged 1,4-Dilithio-2-butene: Structures and Dynamic Behavior. A "T" Shaped Dimeric Cluster in the Solid State

Gideon Fraenkel,* Xiao Chen, Albert Chow, and Judith Gallucci

Department of Chemistry, Ohio State University, 100 W. 18th Avenue, Columbus, Ohio 43210, United States

Supporting Information

ABSTRACT: X-ray crystallographic NMR and calculational modeling studies using B3LYP/6-311G* of selected dilithium derivatives of the 1,3-butadiene dianion including *cis*-dilithio-1,4-bis(TMS)-2-butene·$(TMEDA)_2$ **2**, internally solvated *cis*-dilithio-1,4-bis[bis(2-methoxyethyl)-aminomethyldimethylsilyl]-2-butene **5**, and using only modeling, 1,4-dilithio-2-butene·$(TMEDA)_2$ **9** reveal remarkably similar structural and NMR parameters. In the solid, **5** consists of unusual "T" shaped dynamic clusters. In all three bridging lithiums are sited between 1.8 and 1.9 Å normal to the centroids of opposite faces of the near coplanar of the 2-butene component. Typical bond lengths of the latter are 1.458 ± 0.004, 1.385 ± 0.006, and 1.459 ± 0.003 Å, for C1−C2, C2−C3, and C3−C4, respectively. The ^{13}C chemical shifts lie within the ranges δ 21 ± 0.5, 99 ± 0.7, 99 ± 0.7 and 21 ± 0.5 for C1, C2 and C3 together, and C4, respectively. Dynamic ^{13}C NMR provides activation parameters for nitrogen inversion in **2** and **5**, overall molecular inversion of **5**, and conformational interconversion of **2**.

INTRODUCTION

One of the few simple π conjugated dianions[1] is the result of two electron reduction of 1,3-dienes[2a] or of 1,4-dimetalation of 2-butenes or substituted 2-butenes.[2b−d,3] In related chemistry many 1,3-dienes react cleanly with magnesium metal to form adducts of formula $(1,3\text{-diene}\cdot Mg)_n$.[4] These metal derivatives of the butadiene dianion system have found wide use in organic synthesis.

Questions regarding the nature of 1,3-diene-dianions and their metal derivatives have been treated theoretically.[5] In these treatments the main conclusions regarding the dilithium derivatives include a cisoid bridged dilithium structure with negative charge concentrated at the termini, **1**. Thus the central C2−C3 bond has considerably higher π character compared to the C1−C2 and C3−C4 bonds, respectively.

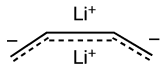

1

These characteristics are common features among X-ray crystallographic results that have been published, for example, for 1,4-dilithio-1,4-diphenyl-2-butene,[6] dilithio bis(trimethylsilyl)-*o*-xylene,[7] and 1,4-dilithio-1,4-bis(trimethylsilyl)-2-butene·$(TMEDA)_2$, **2**.[8]

Interactions that are known to compromise π conjugation include substituent effects and different kinds of geometric distortions such as those due to ring strain and steric effects. In addition we described examples of nominally delocalized ion-paired lithium carbanide salts within which the degree of delocalization depends critically on the relative orientation of anion and cation. For example NMR studies showed externally solvated 1-trimethylsilylallyllithium **3** to be fully delocalized with lithium normal to the centroid of the allyl plane. By contrast X-ray crystallography and NMR studies of its internally

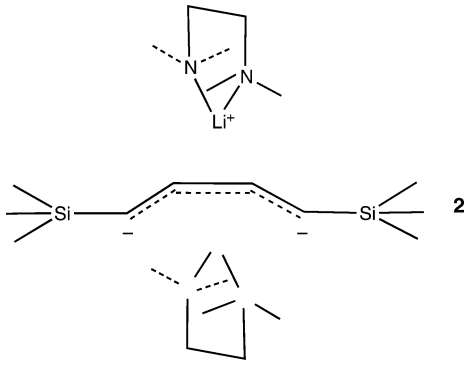

2

coordinated analogue **4** show it to be partly localized.[9] It was proposed that the ligand tether in **4** is too short to place Li normal to the allyl plane at its centroid as in the case of externally solvated **3**. Instead, the ligand in **4** places Li normal to this plane at one of the allyl termini. From this aberrant site

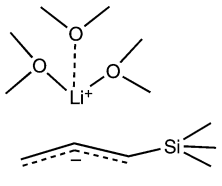

3

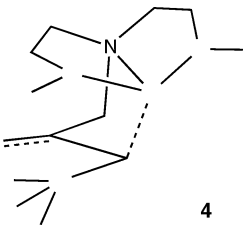

4

electrostatic interactions between Li and the allyl moiety polarize allyl to become partly localized. We have named this effect site specific electrostatic perturbation of conjugation, SSEPOC.[9]

Received: November 28, 2012
Published: January 6, 2013

dx.doi.org/10.1021/jo302439t | J. Org. Chem. 2013, 78, 1149−1156

Herein, to assess the possible operation of SSEPOC on the 1,4-dilithio-1,4-bis(silyl)-but-2-ene system, we now report the results of X-ray crystallographic and NMR studies of potentially internally coordinated 1,4-dilithio-1,4-bis[bis(2-methoxyethyl)-aminomethyldimethylsilyl]-but-2-ene **5** and compare our findings to those reported by Field[8] and our own for its externally solvated analogue 1,4-dilithio-1,4-bis(trimethylsilyl)-but-2-ene-$(TMEDA)_2$, **2**.[8]

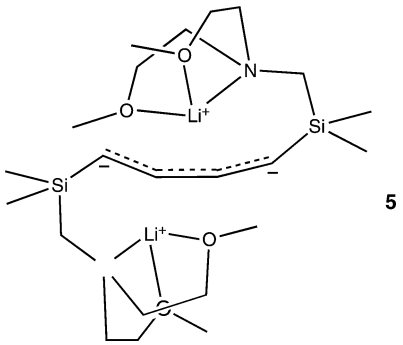

5

RESULTS AND DISCUSSION

Compound **2** was prepared as described in the literature.[8] The synthesis of **5** is outlined below, see **6** → **7** → **8** → **5** (Scheme 1).

Scheme 1

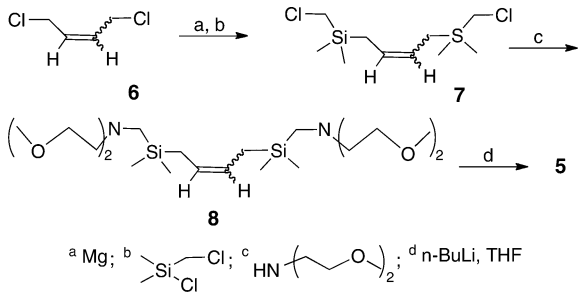

X-ray crystallography of **5** reveals two independent molecules in the same asymmetric unit with very similar structures, and they are labeled **5A** and **5B**. The ORTEP diagram for **5A** is shown in Figure 1a. The unit cell contains two **5A** and two **5B** molecules, and they are arranged as two "T" shaped dimers with **5A** and **5B** occupying, respectively, the horizontal and vertical components of the "T"; see Figure 1b. The shortest separation between the **5A** and **5B** molecules within the **5A·5B** dimer is 2.883 Å, between C13A and a hydrogen on C14B, which is close to the van der Waals radius sum of 2.8 Å. Both **5A** and **5B** have essentially the same geometrical features. While several aromatic compounds have been claimed to assemble into "T" shaped clusters,[10] as of this writing there have been no reports of dimeric "T" shaped molecular structures in the solid state based on X-ray crystallography. However in the case of **5A** and **5B** large negative charges at the butenediyl termini may well facilitate the "T" shaped dimer to reduce intermolecular repulsion. Such "T" shaped arrangements are not observed in the unit cell of **2**.[8]

For comparison purposes selected structural parameters for compounds **2** and **5A** are displayed in Figures 2 and 3, respectively. These two compounds have several structural features in common. The butenediyl units in each are cisoid and near coplanar. Both are lithium bridged with lithium atoms normal to the centroids on opposite faces of the C1, C2, C3, and C4 near planes. The distances of the lithium atoms from the least-squares plane through the atoms C1, C2, C3, and C4, as numbered in Figure 3 are not significantly different in **5A** and **5B** and are as follows: For Li1A and Li2A of **5A** and for Li1B and Li2B of **5B** the distances are 1.871(5), 1.863(5), 1.866(5), and 1.877(5), respectively, all in Å. For the equivalently sited lithium atoms in **2** the distances are both 1.81 Å by symmetry.

In compound **2** each lithium is bidentately coordinated to a single TMEDA, while in **5A** and **5B** the entire species is internally solvated with each lithium tridentately coordinated to a single pendant ligand. The butenediyl bond lengths are also remarkably similar. They are for **2** in the order C1−C2, C2−C3, and C3−C4, 1.49(3), 1.34(3), and 1.45(3), respectively, all in Å, whereas for **5A** the corresponding values, in the same order, are 1.454(4), 1.372(4), and 1.454(4) and for **5B** they are 1.465(4), 1.378(4), and 1.457(4) also all in Å. These results imply that **2** and **5A** and **5B** have similar electronic structures. The main difference between the internally solvated **5A** and **5B** and externally solvated **2** two lies in the orientation of the terminal butenediyl silicon bonds. In **2** these are nearly coplanar with the butenediyl moiety, whereas in **5A** and **5B** the corresponding bonds are bent externally on opposite sides with respect to the butenediyl plane. This places the two silicons in **5A** and **5B** ca. 0.8 Å normal to opposite faces of the butenediyl plane. Thus in **5A** Si1A and Si2A are −0.788(1) Å and 0.814(1) Å, respectively, from the plane through C1A, C2A, C3A, and C4A, whereas for **5B** the corresponding values for Si1B and Si2B are, respectively, −0.794(1) Å and 0.829(1) Å from the plane through C1B, C2B, C3B, and C4B. The associated torsional angles are Si1A, C1A, C2A, C3A, 151.1(2)°; C2A, C3A, C4A, Si2A, 149.1(2)°; Si1B, C1B, C2B, C3B 150.8(3)°; C2B, C3B, C4B, Si2B, 149.5(2)°. Thus it appears that the arrangement of the silicons in **2** and **5A** and **5B** accommodates the core dilithio butenediyl unit in these species to a common framework. The bending of Si1−C2 and Si2−C4 bonds from the butenediyl plane is also responsible for the chiral character of **5A** and **5B**.

It is also of note that in both **5A** and **5B** the distances from lithium to the terminal butenediyl carbons are different. Thus where silicon and lithium are on the same side of the butenediyl plane the larger lithium terminal butenediyl carbon separation is to the carbon directly bonded to the latter silicon. For example in **5A** Li2A is closer to C1A than to C4A the separations being C1A−Li2A = 2.400(5) Å and C4A−Li2A = 2.447(5) Å. In similar fashion Li1A is closer to C4A than to C1A with separations C4A−Li1A = 2.412(6) Å and C1A−Li1A = 2.446(5) Å. Similar effects apply to **5B**. This effect is clearly due to cisoid steric repulsions between lithium and the adjacent silicon.

At room temperature the C2 and C3 ^{13}C resonances of **2** in diethyl ether-d_{10} solution give rise to a single sharp line. On cooling of the sample this resonance progressively broadens, and by 160 K it resolved into a 1:2:1 triplet, see Figure 4. The corresponding resonances for the terminal butenediyl carbons behave in a similar fashion. A possible interpretation of these results may be that compound **2** actually consists of two interconverting species in diethyl ether-d_{10} solution, the 1,4-(exo,exo) structure reported previously[8] and a second one assigned as 1,4-(endo,exo), as proposed in Figure 5.

dx.doi.org/10.1021/jo302439t | J. Org. Chem. 2013, 78, 1149−1156

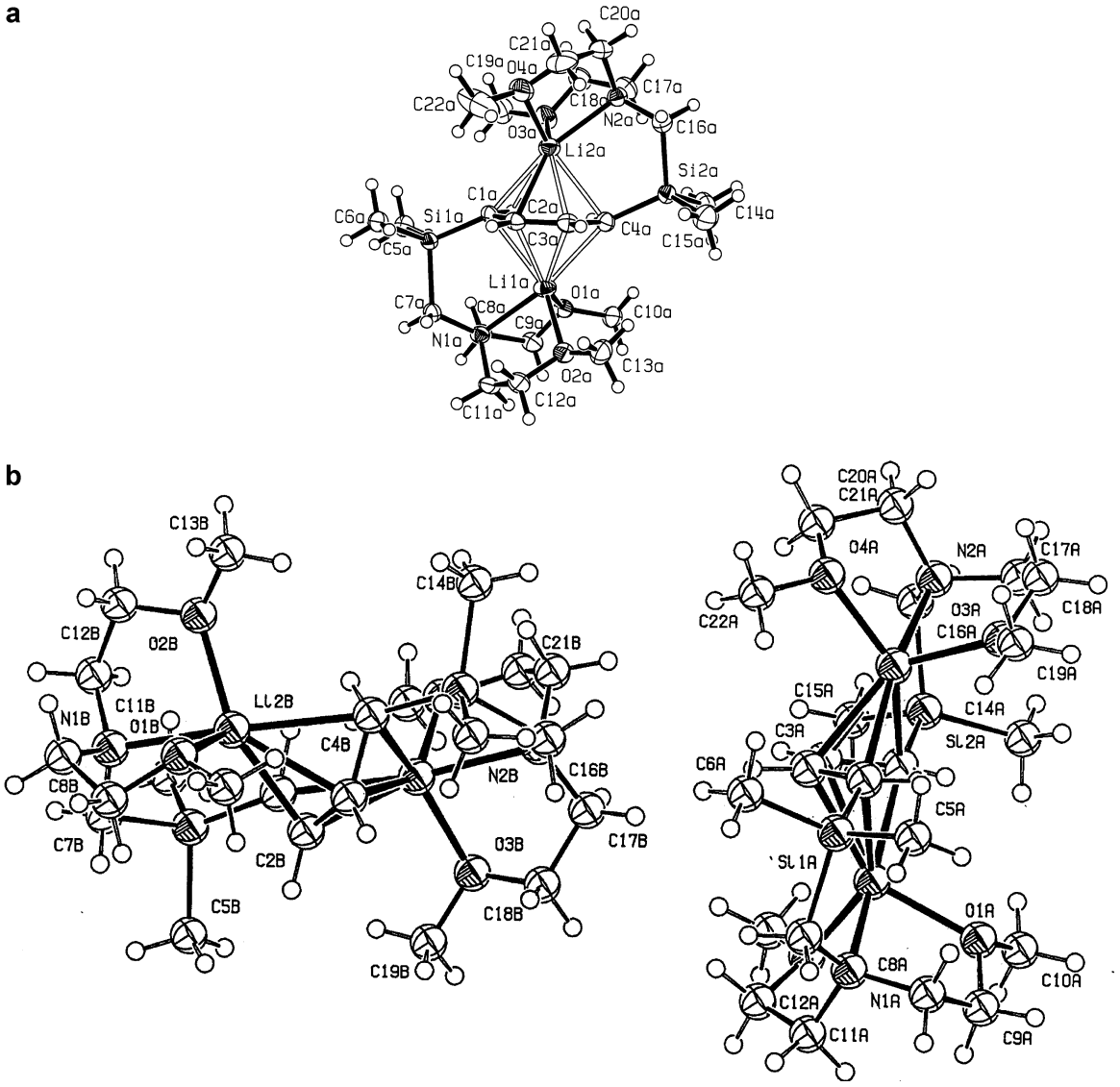

Figure 1. (a) ORTEP diagram of **5A**. (b) ORTEP diagram of the **5A·5B** cluster.

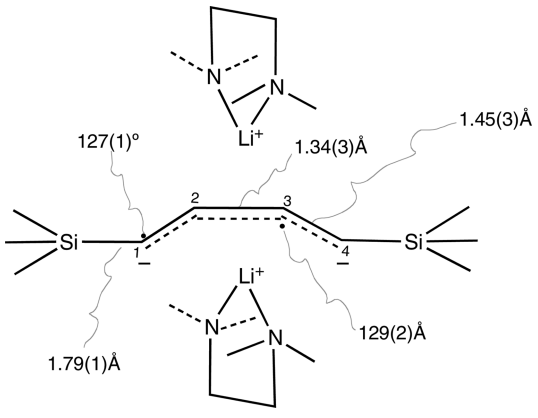

Figure 2. Compound **2** with selected X-ray crystallographical structural parameters taken from ref 8.

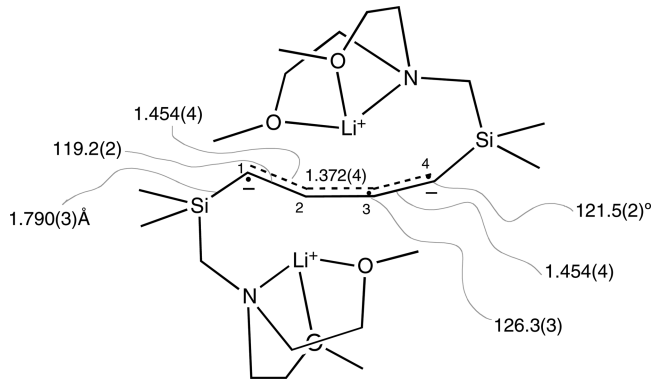

Figure 3. Compound **5A** with selected X-ray crystallographic bond lengths (Å) and angles (deg). Li_1 and Li_2 butenediyl centroid separations are 1.875(5) and 1.863(5) Å, respectively.

Proposed chemical shifts assigned for **2-(1,4-exo,exo)** and **2-(1,4-endo,exo)** are listed around the two butenenedyil frameworks in Figures 6 and 7, respectively. In our assignment of **2-(1,4-endo,exo)** the "U" shaped butenediyl is maintained to maximize electrostatic attractions between the lithiums and the negatively charged terminal butenediyl carbons. Then interconversion between **2-(1,4-exo,exo)** and **2-(1,4-endo,exo)** would take place via rotations around the terminal

dx.doi.org/10.1021/jo302439t | J. Org. Chem. 2013, 78, 1149−1156

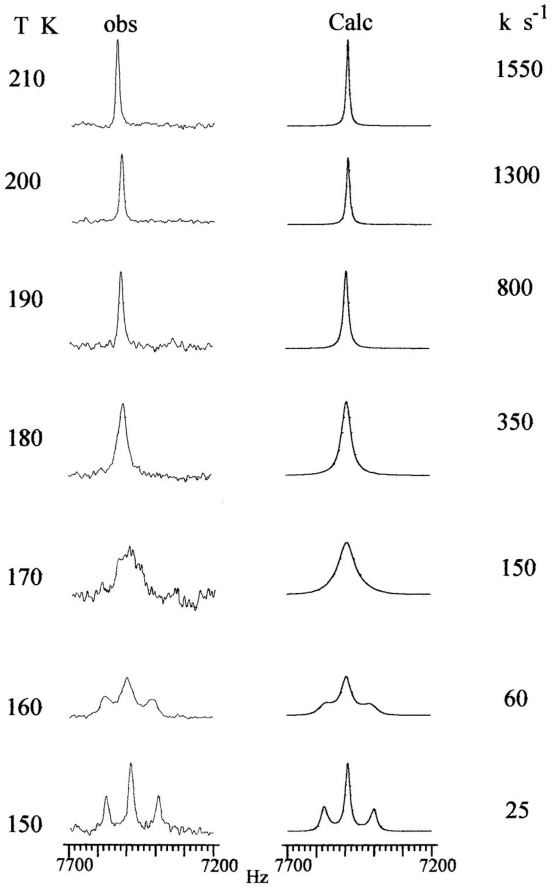

Figure 4. Compound **5** at 0.4 M concentration in THF-d_8 solution. ^{13}C NMR line shapes for C2 and C3 (left) observed at different temperatures, K, and (right) calculated to fit with first-order rate constants.

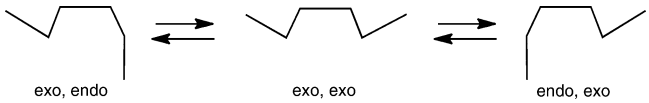

Figure 5. Interconversion scheme of **2-(1,4-endo,exo)** with **2-(1,4-exo,exo)**, carbon framework of bonds.

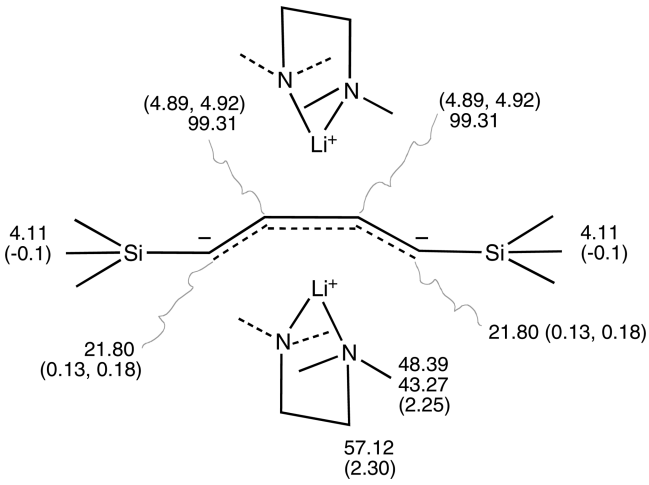

Figure 6. Compound **2** at 0.2 M concentration in diethyl ether-d_{10} at 160 K, ^{13}C and (^{1}H) NMR shift assignments for **2-(1,4-exo,exo)**, δ units.

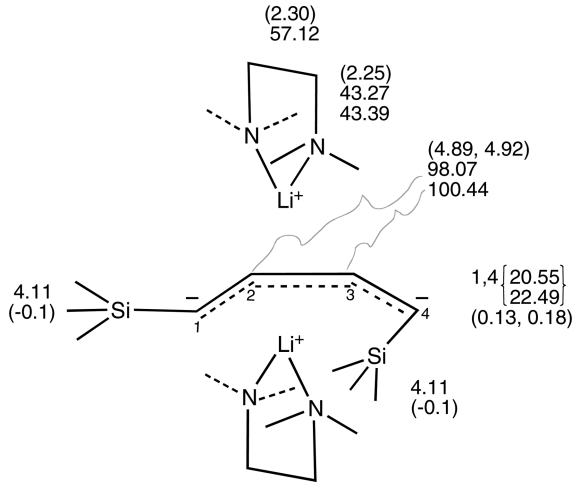

Figure 7. Compound **2** at 0.2 M concentration in diethyl ether-d_{10} at 160 K, ^{13}C and (^{1}H) NMR shift assignments for **2-(1,4-endo,exo)**, δ units.

butenediyl carbon carbon single bonds, one at a time as proposed in Figure 5. Selected ^{13}C and proton NMR shifts for **5** in THF-d_8 are listed around the structure in Figure 8. Note

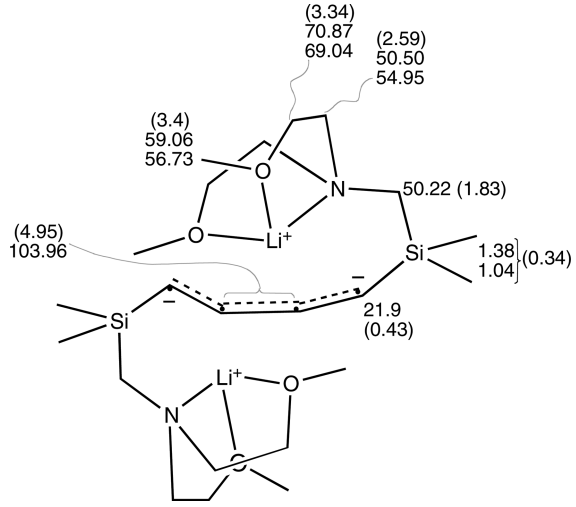

Figure 8. Compound **5** at 0.2 M concentration in THF-d_8 at 200 K, ^{13}C and (^{1}H) NMR shifts, δ units.

that while compound **5** consists of two slightly different structures in the solid state, solution NMR displays just one set of chemical shifts. This is not unreasonable since the "T" shaped cluster would not be expected to prevail in THF-d_8 solution. Besides, even it were stable in solution the structures and **5A** and **5B** are so similar that ^{13}C chemical shift differences between would be too small to detect.

The ^{13}C shifts interpreted for the butenediyl moieties of **2-(1,4-exo,exo)** and **2-(1,4-endo,exo)** and **5** are remarkably similar; see Figures 6, 7, and 8. Those for C2 and C3 lie well within the range 100 ± 1 δ while the terminal butenediyl shifts are all within 21 ± 1 δ. These values are consistent with the C2−C3 π bond and single bonds for C1−C2 and C3−C4 revealed by the X-ray crystallographic data for **2-(1,4-exo,exo)**, **5A**, and **5B**. Our proton shifts for the conformers of **2** in diethyl ether-d_{10} are very similar to those reported by Field using benzene-d_6 solutions.[8] However Field reported only a single

dx.doi.org/10.1021/jo302439t | J. Org. Chem. 2013, 78, 1149−1156

Table 1. Structural Features, Observed and Calculated, for Compounds 2, 5, and 9

				5A	5B	5A	5B
	2, X-ray[8]	**2**, B3LYP/6-311G*	**9**, B3LYP/6-311G*	X-ray		B3LYP/6-311G*	
			Bond Lengths (Å)				
1, 2	1.45(3)	1.4569	1.4555	1.454(4)	1.465(4)	1.4592	1.4578
2, 3	1.33(3)	1.3895	1.3974	1.372(4)	1.378(4)	1.3859	1.3859
3, 4	1.45(3)	1.4620	1.4530	1.454(4)	1.457(4)	1.4688	1.4593
			Li Centroid Separation (Å)				
1.81		1.86	1.86	1.866(5)	1.821(5)	2.0501	1.8711
1.81		1.86	1.94	1.877(5)	1.863(6)	1.8736	2.0880
			Mulliken Charges				
CA							
1		−0.879	−0.7184			−0.8932	−0.8271
2		−0.323	−0.336			−0.3388	−0.3348
3		−0.330	−0.3110			−0.3354	−0.3379
4		−0.879	−0.7181			−0.8278	−0.8329
			Natural Charges				
1		−1.1805	−0.9299			−1.1050	−1.1044
2		−0.4211	−0.4799			−0.3656	−0.3614
3		−0.4474	−0.4535			−0.3637	−0.3672
4		−1.1203	−0.9228			−1.1039	−1.1069

conformer and that ^{7}Li NMR of **2** in benzene-d_6 solution at room temperature displayed triplet splitting of 1.5 Hz due to ^{7}Li spin coupling to the terminal butenediyl hydrogens.[8] This assignment was confirmed by means of proton decoupling.[8] By contrast our sample in diethyl ether-d_{10} did not display such spin coupling down to 160 K. Its absence could not be due to fast ^{7}Li nuclear electric quadrupole induced relaxation since the ^{7}Li NMR of this sample consisted of a single sharp line down to 160 K. It is conceivable that fast bimolecular mutual exchange of lithiums between **2**'s might be responsible for the absence of observable ^{7}Li proton spin coupling. The rate of this mutual exchange would have to be fast relative to the NMR time scale in diethyl ether-d_{10} even at 160 K but slow in benzene up to room temperature.[8]

The results of modeling calculations on the systems reported herein using B3LYP/6-311G*[12,13] are almost identical to those observed and reveal some interesting common features. These results are compared with the experimental ones in Table 1. Thus, starting with its X-ray parameters compound **2** (exo,exo) was modeled as a monomeric gas phase species. Optimization produced only the 1,4-(exo,exo) conformer of **2** described above. The final optimized geometry is stable as based on frequency calculation. Calculated structural parameters and ^{13}C shifts using GIAO are almost the same as those observed experimentally. See Table 2.

Table 2. ^{13}C Chemical Shifts (δ) of 2, 5, and 9, Observed and Calculated

	2 obsd[a]		**2** calcd[b]				
C	exo,exo	endo,exo	exo,exo	**9** calcd[b]	**5** obsd[c]	**5A** calcd[b]	**5B** calcd[b]
1	21.80	20.55	20.46	14.90	21.90	19.31	19.01
2	99.31	98.07	93.16	97.49	103.37	100.14	100.63
3	99.31	100.44	99.94	99.98	103.37	100.05	99.43
4	21.80	23.47	20.16	13.63	21.90	19.05	20.22

[a]In diethyl ether-d_{10}. [b]B3LYP/6-311G*. [c]In THF-d_8.

In similar fashion, modeling **5A** and **5B**, first as the "T" shaped cluster and then separately, reveal results almost identical to those observed from X-ray crystallography, Tables 1 and 2. Finally, to acquire some insight into the role of TMS in structures **2**, **5A**, and **5B**, we were interested in obtaining the parent compound, TMEDA complexed dilithio butenediyl, **9**. We were unable to prepare this compound pure. However we have modeled it in similar fashion to those described above, using published structural parameters for **2**[8] and then replacing the TMS groups with hydrogens. Selected resulting structural parameters and ^{13}C butenediyl shifts are listed around the structure in Figure 9. These values are remarkably close to

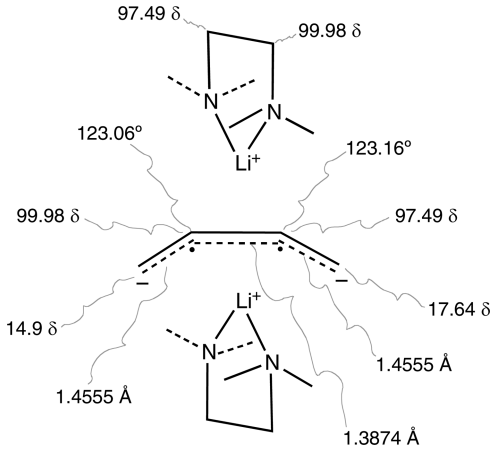

Figure 9. Compound **9** modeled using B3LYP/6-311G*; calculated bond lengths (Å), bond angles (deg), and ^{13}C shifts (δ); Li centroid separations are upper 1.860 Å and lower 1.814 Å.

those both observed and calculated for **2**, **5A**, and **5B**. All species investigated experimentally and by calculation show the same butenediyl bond lengths, similar lithium centroid separations, almost identical ^{13}C NMR shifts, and by calculation very similar Mulliken and natural charges, Table 1. Apparently silicon substitution has very little influence on the structure of the core dilithio butenediyl moiety. Thus it appears that among

dx.doi.org/10.1021/jo302439t | J. Org. Chem. 2013, 78, 1149−1156

the results described herein and published so far for salts of the dilithium butenediyl system, the dilithium butendyl unit has the same structure throughout.

Compounds **2** and **5** exhibit some interesting changes of NMR line shape due to different molecular reorganization processes. As noted above, on the basis of ^{13}C NMR line shapes of **2** in diethyl ether-d_{10} at 160 K and averaging effects with temperature, Figure 4, we proposed that **2** in solution consists two interconverting rotamers, **2-(1,4-endo,exo)** and **2-(1,4-exo,exo)**, the rates of interconversion increasing with temperature; see Figure 5. Using the scheme in Figure 5 NMR line shape analysis of the averaging butenediyl ^{13}C resonances of **2**, shown in Figure 4, gives rise to the activation parameters for **2-(1,4-exo,exo)** interconverting with **2-(1,4-endo,exo)** listed in Table 3. In addition, ^{13}C NMR of TMEDA coordinated to **2** also undergoes changes in line shape with temperature. Thus the 1:1 doublet observed for the geminal N-methyls at 150 K progressively averages with increasing temperature to a single line by 230 K. These changes are most likely the result of fast reversible N–Li dissociation accompanied by inversion at nitrogen. NMR line shape analysis yields the activation parameters listed in Table 3.

Table 3. Compound 2 in Diethyl Ether-d_{10}. Activation Parameters for Nitrogen Inversion (1) and Interconversion between 2-(exo,exo) and 2-(endo,exo) (2 and 3)

no.	^{13}C resonance	$\Delta H^{\ddagger}$ (kcal mol^{-1})	$\Delta S^{\ddagger}$ (eu)
1	$N(CH_3)_2$	6.7 ± 1	−6.4 ± 0.8
2	C1, C2	4.2 ± 0.5	−22 ± 2
3	C2, C3	4.2 ± 0.5	−22 ± 2

Changes in ^{13}C NMR lineshapes were also observed for compound **5**. Carbon-13 and proton shifts observed for **5** in THF-d_8 solution at 200 K are listed around the structure in Figure 8. Doublet splitting observed for the geminal methyl ^{13}C NMR supports the chiral structure of **5**. With increasing temperature this doublet progressively averages to a single line by 280 K. Such averaging is diagnostic of overall molecular inversion as proposed in Figure 10. Most likely it is the overall result of transfer of coordinated lithiums between faces of the butenediyl plane. Thus, NMR line shape analysis of changes in the geminal methyl ^{13}C resonance yielded the dynamics of overall inversion of **5**. The resulting activation parameters are listed in Table 4.

In addition to revealing overall inversion of **5**, NMR also provided kinetic evidence for separate inversion at nitrogen. At low temperature, 200 K, all carbons within a ligand are magnetically nonequivalent. However the two pendant ligands within **5** have the same set of ^{13}C chemical shifts. Thus at low temperature we observe clean 1:1 ^{13}C doublets for methoxy, OCH_2, and $N(CH_2CH_2O)$ carbons, respectively. With increasing temperature each of these doublets progressively averages to a single line at its respective center. NMR line shape analysis of all these averaging doublets due to the ligand carbons gives rise to the same specific rates. The resulting activation parameters are listed in Table 4. These effects are most likely the result of fast reversible ligand lithium dissociation accompanied by inversion at nitrogen.

Table 4. Compound 5 in THF-d_8. Activation Parameters for Inversion at Nitrogen (1–3) and Overall Inversion (4)

no.	^{13}C resonance	$\Delta H^{\ddagger}$ (kcal mol^{-1})	$\Delta S^{\ddagger}$ (eu)
1	OCH_3	7.4 ± 1	−14 ± 2
2	OCH_2	7.4 ± 1	−15 ± 2
3	NCH_2CH_2O	7.2 ± 1	−15 ± 2
4	$Si(CH_3)_2$	6.5 ± 0.8	−24 ± 3

While we can recognize the overall reorganization processes responsible for these changes in NMR line shapes, the detailed mechanisms of these processes are still unknown. It is attractive to speculate that partial localization of the butenediyl dianion moiety **10**, to delocalized allyl anion with localized C^-, **11**, may have a role in some of these reorganizations, see **10** → **11**, without substituents.

Interestingly our $\Delta H^{\ddagger}$ values are close to the crude Huckel estimate of 7.5 kcal/mol for the transformation **10** → **11**.

CONCLUSIONS

In summary, the results presented herein demonstrate the integrity of the di-Li^+ bridged cisoid butenediyl dianion whose structural features appear to be independent of the nature of Li^+ coordination and of silicon substitution. In the solid state internally coordinated **5** assembles into "T" shaped dimeric clusters, one of few such definitively established examples. These systems undergo fast equilibrium molecular reorganizations.

EXPERIMENTAL SECTION

(*cis*,*trans*)-1,4-Bis(chloromethyldimethylsilyl)but-2-ene, 7. A solution of (*cis*,*trans*)-1,4-dichlorobut-2-ene. (8.9 g, 71 mmol) in THF (20 mL) was added to a suspension of magnesium powder grade 4

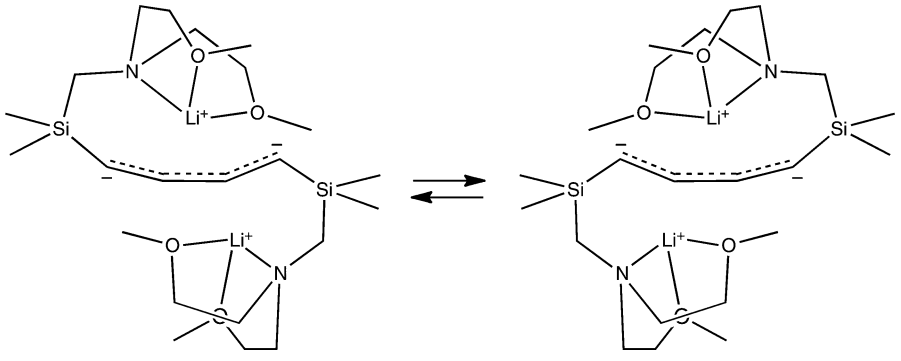

Figure 10. Overall inversion of compound **5**.

dx.doi.org/10.1021/jo302439t | J. Org. Chem. 2013, 78, 1149–1156

(3.5 g, 144 mmol) in dry freshly distilled THF (200 mL) at a rate consistent with maintaining the reaction temperature at 50−60 °C. The mixture was stirred at 60 °C for 48 h until the magnesium powder almost disappeared. The mixture was cooled to 0 °C with an ice bath, chloro(chloromethyl)dimethylsilane (18 g, 128 mmol) was added, and the mixture was stirred for 1 h at room temperature. Then 100 mL of ice−water was added dropwise with ice bath cooling. The products were extracted into diethyl ether (3 × 50 mL). The combined extracts were dried over $NaSO_4$ and filtered, and the solvent was removed in vacuo. Distillation of the residue bp 82−86 °C/0.5 Torr gave 7.6 g of the title compound as a colorless liquid in 44.7% yield. ^{1}H NMR ($CDCl_3$, 250 MHz, δ): 0.08, 0.10 (bs, 12H, $SiMe_2$), 1.52, 1.55 (bd, 4H, $H^{1,4}$), 2.75 2.77 (bs, 4H, CH_2Cl), 5.26, 5.30 (bm, 2H, $H^{2,3}$). ^{13}C NMR ($CDCl_3$, 62.9 MHz, δ): −4.9, −4.7 ($SiMe_2$), 14.8, 19.6 ($C^{1,4}$), 29.9, 30.0 (CH_2Cl, 122.8, 124.1 ($C^{2,3}$).

(*cis,trans*)-1,4-Bis[bis(2-methoxyethyl)aminomethyldimethylsilyl]but-2-ene, 8. Under an argon atmosphere, bis(2-methoxyethyl)amine (4 g, 30 mmol) and a mixture of *cis*- and *trans*-1,4-bis(chloromethyldimethysilyl)but-2-ene (2.02 g, 7.5 mmol) were introduced into a 50 mL round-bottomed flask equipped with a magnetic stir bar and reflux condenser. The mixture was heated to 120 °C and stirred for 4 days. Then 10 mL of 2 N aqueous KOH was added. The mixture was extracted with $CHCl_3$ (3 × 25 mL). The $CHCl_3$ layers were combined and washed with saturated aqueous NaCl solution and dried with $NaSO_4$. After filtration, the solvent was removed in vacuo. Column chromatography gave 2.42 g of the title compound as a red liquid in 69.8% yield. ^{1}H NMR ($CDCl_3$, 250 MHz, δ): 0.02, 0.04 (bs, 12H, $SiMe_2$), 1.42 1.44 (d, 4H, $H^{1,4}$), 2.08, 2.10 (d, 4H, $SiCH_2N$), 2.66 (t, 8H, NCH_2). 3.30 (s, 12H, OCH_3), 3.45 (t, 8H, CH_2O), 5.19, 5.28 (bt, 2H, $H^{2,3}$). ^{13}C NMR ($CDCl_3$, 62.9 MHz, δ): −3.2, −3.0 ($SiMe_2$), 16.4, 21.3 ($C^{1,4}$), 45.9 ($SiCH_2N$), 57.3 (NCH_2), 58.8 (OCH_3), 70.9 (CH_2O), 123.1, 124.4 ($C^{2,3}$).

1,4-Dilithio-1,4-bis[bis(2-methoxyethyl)aminomethyldimethylsilyl]but-2-ene, 5. A 10 mL Schenk tube equipped with a magnetic stir bar and argon inlet tube was flame-dried under vacuum and flushed with argon. Freshly distilled dry diethyl ether (2 mL) and a solution of *n*-BuLi in hexane (1.32 mL, 1.6 M, 2.1 mmol) was added by syringe. After cooling the solution to −78 °C with a dry ice/acetone bath. (*cis, trans*)-1,4-Bis[bis(2-methoxyethyl)aminomethyldimethylsilyl]but-2-ene (0.462 g, 1.0 mmol) was introduced slowly by syringe. After 30 min at room temperature the solution turned deep red. After stirring overnight the solution was concentrated in vacuo, washed with pentane (3 × 4 mL), and then dried in vacuo. A 0.2 M solution of **5** in THF-d_8 was prepared for NMR studies. ^{1}H NMR (THF-d_8, 250 MHz, δ): −0.1(12H, s, $SiMe_2$), 0.43 (2H, m, $H^{1,4}$), 1.83 (4H, br, $SiCH_2N$), 2.59 (8H, br, NCH_2), 3.34 (8H, t, CH_2O), 3.40 (12H, s, OCH_3), 4.98 (2H, m, $H^{2,3}$). ^{13}C NMR (THF-d_8, 75.5 MHz, δ): 0.3 ($SiMe_2$), 22.0 ($C^{1,4}$), 50.2 ($SiCH_2N$), 55.2 (NCH_2), 57.4 (OCH_3), 69.6 (CH_2O), 103.4 ($C^{2,3}$). ^{7}Li NMR (THF-d_8, 116.6 MHz, δ): 1.71.

CALCULATIONS

Models of **2**, **5**, and **9** have been calculated at the MPWPW91 and B3LYP levels of theory starting with basis set 3-21G and building up to 6-311G* using starting parameters from published crystallographic data. Optimized structures were confirmed as stable ground state structures with the usual frequency calculations.[12,13] Given the MPWPW91 and B3LYP results ^{13}C NMR shifts were then calculated using GIAO.[14]

ASSOCIATED CONTENT

Supporting Information

NMR, X-ray crystallographic, and calculational data. This material is available free of charge via the Internet at http://pubs.acs.org.

AUTHOR INFORMATION

Corresponding Author

*E-mail: fraenkel@mps.ohio-state.edu.

Notes

The authors declare no competing financial interest.

ACKNOWLEDGMENTS

This research was generously supported by the National Science Foundation and by the M. S. Newman Chair of Chemistry. This article is dedicated to the memory of Dr. Charles Cottrell.

REFERENCES

(1) (a) Thompson, C. M. *Dianion Chemistry in Organic Synthesis*; G. R. C. Press: Ann Arbor, MI, 1993; Chapter 2. (b) Barry, C. E., III; Bates, R. B.; Beavers, W. H.; Camu, F. A.; Gordon, B., III; Hsu, H. F. J.; Mills, N. S.; Ogle, C. A.; Siahaan, T. J.; Suvanachut, K.; Taylor, S. R.; White, J. J.; Yager, K. M. *Synlett* **1991**, 207. (c) Bates, R. B.; Ogle, C. A. *Carbanion Chemistry*; Springer Verlag: Heidelberg, 1983.

(2) (a) Weyenberg, D. R.; Toporcer, L. H.; Nelson, L. E. *J. Org. Chem.* **1968**, *33*, 1975. (b) Bates, R. B.; Beavers, W. A.; Greene, M. G.; Klein, J. H. *J. Am. Chem. Soc.* **1974**, *96*, 5640. (c) Klein, J. *Tetrahedron* **1988**, *44*, 503−518. (d) Bates, R. B.; Hess, B. A.; Ogle, C. A.; Schaad, L. J. *J. Am. Chem. Soc.* **1981**, *103*, 5052.

(3) Bahl, J. J.; Bates, R. B.; Beavers, W. A.; Mills, N. A. *J. Org. Chem.* **1976**, *41*, 1620.

(4) (a) Xiong, H.; Rieke, R. D. *J. Org. Chem.* **1989**, *54*, 3247. (b) Erker, G.; Kruger, C.; Muller, G. *Adv. Organomet. Chem.* **1985**, *24*, 1. (c) Yasuda, H.; Tasumi, K.; Nakamura. *Acc. Chem. Res.* **1985**, *18*, 120. (d) Walther, D.; Pfeutretenreuter, C. *Naturwiss. Reinhe.* **1985**, 789. (e) Rieke, R. D.; Sell, M. S.; Xiong, H. *J. Org. Chem.* **1995**, *60*, 5143−5149.

(5) (a) Kos, A. J.; Stein, P.; Schleyer, P. v. R. *J. Organomet. Chem.* **1985**, *280*, C1−C5. (b) Kos, A. J.; Schleyer, P. v. R. *J. Am. Chem. Soc.* **1980**, *102*, 7928−7929. (c) Sommerfeld, T. *J. Am. Chem. Soc.* **2002**, *124*, 1119−1124. (d) Bates, R. B.; Hess, B. A.; Ogle, C. A.; Schaad, L. J. *J. Am. Chem. Soc.* **1981**, *103*, 5052. (e) Schleyer, P. v. R.; Kos, A. J.; Wilhelm, D.; Clark, T.; Boche, G.; Decker, G.; Etzrodt, H.; Dietrich, H.; Mahdi, W. *J. Chem. Soc., Chem. Commun.* **1984**, 1485−1486. (f) Schleyer, P. v. R.; Clark, T.; Kos, A.; Spitznagel, G. W.; Rohde, C.; Arad, D.; Houk, K. N.; Rondan, N. G. *J. Am. Chem. Soc.* **1984**, *106*, 6467.

(6) Wilhelm, D.; Clark, T.; Schleyer, P. v. R.; Dietrich, H.; Mahdi, W. *J. Organomet. Chem.* **1985**, *280*, C6−C10.

(7) Lappert, M. F.; Raston, C. L.; Skelton, B. W.; White, A. H. *J. Chem. Soc. Chem. Commun.* **1982**, 11 describes systems wherein the butenediyl moiety is incorporated within aromatic structures..

(8) (a) Field, L. D.; Gardiner, M. G.; Messerle, B. A.; Raston, C. L. *Organometallics* **1992**, *11*, 3566−3570. (b) Field, L. D.; Gardiner, M. G.; Kenard, C. H.; Messerle, B. A.; Raston, C. L. *Organometallics* **1991**, *10*, 3167.

(9) (a) Fraenkel, G.; Cabral, J.; Chen, X.; Ren, Y. *J. Org. Chem.* **2009**, *74*, 2311−2320. (b) Fraenkel, G.; Gallucci, J.; Liu, H. *J. Am. Chem. Soc.* **2006**, *128*, 8211. (c) Fraenkel, G.; Chen, X.; Gallucci, J. *J. Am. Chem. Soc.* **2008**, *130*, 4140−4145. (d) Fraenkel, G.; Chow, A.; Fleischer, R.; Liu, H. *J. Am. Chem. Soc.* **2004**, *126*, 3983. (e) Fraenkel, G.; Duncan, J. H.; Wang, J. *J. Am. Chem. Soc.* **1999**, *121*, 432−443. (f) Fraenkel, G.; Qiu, F. *J. Am. Chem. Soc.* **1997**, *119*, 3571−3577.

(10) (a) Podeszwa, R.; Szalewicz, K. *Phys. Chem. Chem. Phys.* **2008**, *10*, 2735−2736. (b) Pritchard, D. G.; Nandi, R. N.; Muenter, J. S. *J. Chem. Phys.* **1988**, *89*, 115−123. (c) Seminario, J. M.; Zacarias, A. G.; Tour, J. M. *J. Am. Chem. Soc.* **1998**, *120*, 3970−3974.

(11) (a) Gunther, H.; Moskau, D.; Schmalz, D. *Angew. Chem., Int. Ed. Engl.* **1987**, *26*, 1212. (b) Feigel, M.; Schleyer, P. v. R. *J. Am. Chem. Soc.* **1990**, *112*, 8776. (c) Yu, C.; Levy, G. C. *J. Am. Chem. Soc.* **1984**, *106*, 6533. (d) Bauer, W.; Clark, T.; Schleyer, P. v. R. *J. Am. Chem. Soc.*

1987, *109*, 970. (e) Bauer, W.; Muller, G.; Pi, R.; Schleyer, P. v. R. *Angew. Chem., Int. Ed. Engl.* **1986**, *25*, 1103.
(12) (a) Becke, A. D. *J. Chem. Phys.* **1993**, *98*, 5648−5652. (b) Lee, C.; Yang, W.; Parr, R. G. *Phys. Rev.* **1998**, *B37*, 785−789. (c) Vaska, S. H.; Wilk, L.; Nusair, M. *Can. J. Chem.* **1980**, *58*, 1200−1211. (d) Stephens, P. J.; Devlin, F. J.; Chabalowski, C. F.; Frisch, M. J. *J. Phys. Chem.* **1994**, *98*, 11623−11627.
(13) (a) McLean, A. D.; Chandler, G. S. *J. Chem. Phys.* **1980**, *72*, 5639−5648. (b) Raghavachari, K.; Binkley, J. S.; Seeger, R.; Pople, J. A. *J. Chem. Phys.* **1980**, *72*, 650−654.
(14) (a) London, F. J. *J. Phys. Radium* **1937**, *8*, 394−409. (b) McWeeny, R. *Phys. Rev.* **1962**, *126*, 1028. (c) Ditchfield, R. *Mol. Phys.* **1974**, *27*, 789−807. (d) Wolinsky, K.; Hilton, J. K.; Pulay, P. *J. Am. Chem. Soc.* **1990**, *112*, 8251−8260. (e) Cheeseman, J. R.; Trucks, J. W.; Frisch, M. J. *J. Chem. Phys.* **1996**, *104*, 5497−5509.